Journal of Biomechanical Engineering. Received April 25, 2019;
Accepted manuscript posted October 28, 2019. doi:10.1115/1.4045283

Stribeck Curve Analysis of Temporomandibular Joint Condylar Cartilage and Disc

Jill M. Middendorf[1], Shaden A. Albahrani[2], Lawrence J. Bonassar[1,3]

[1]Sibley School of Mechanical and Aerospace Engineering Cornell University, Ithaca, NY; [2]Department of Chemical Engineering, Virginia Polytechnic Institute and University, Blacksburg, VA; [3]Meinig School of Biomedical Engineering Cornell University, Ithaca, NY;

*Address Correspondence to:
Lawrence J. Bonassar, PhD.
Professor
Department of Biomedical Engineering
149 Weill Hall
Cornell University
Ithaca, NY 14853
(607) 255-9381
lb244@cornell.edu

Submission for the 2019 Annual Educational Issue of the Journal of Biomechanical Engineering (World Congress of Biomechanics Student Award Paper)

Key Words TMJ, Friction, fibrocartilage, lubrication, tribology

Journal of Biomechanical Engineering. Received April 25, 2019;
Accepted manuscript posted October 28, 2019. doi:10.1115/1.4045283

Abstract

Temporomandibular joint (TMJ) diseases such as osteoarthritis and disc displacement have no permanent treatment options, but lubrication therapies, used in other joints, could be an effective alternative. However, the healthy TMJ contains fibrocartilage, not hyaline cartilage as is found in other joints. As such, the effect of lubrication therapies in the TMJ is unknown. Additionally, only a few studies have characterized the friction coefficient of the healthy TMJ. Like other cartilaginous tissues, the mandibular condyles and discs are subject to changes in friction coefficient due to fluid pressurization. In addition, the friction coefficients of the inferior joint space of the TMJ are affected by the sliding direction and anatomic location. However, these previous findings have not been able to identify how all 3 of these parameters (anatomic location, sliding direction, and fluid pressurization) influence changes in friction coefficient. This study used Stribeck curves to identify differences in the friction coefficients of mandibular condyles and discs based on anatomic location, sliding direction, and amount of fluid pressurization (friction mode). Friction coefficients were measured using a cartilage on glass tribometer. Both mandibular condyle and disc friction coefficients were well described by Stribeck curves (R^2 range 0.87 – 0.97; $p < 0.0001$). These curves changed based on anatomic location ($\Delta\mu \sim 0.05$), but very few differences in friction coefficients were observed based on sliding direction. Mandibular condyles had similar boundary mode and elastoviscous mode friction coefficients to the TMJ disc ($\mu_{min} \sim 0.009$ to 0.19) and both were lower than hyaline cartilage in other joints (e.g.: knee, ankle, etc.). The observed differences here indicate that the surface characteristics of each anatomic region cause differences in friction coefficients.

Introduction

Temporomandibular joint (TMJ) diseases, including osteoarthritis and disc displacement, collectively affect about 25% of the population [1–3], and have been linked to increased friction in the joint [4–6]. Since TMJ disease has no effective and durable treatment options, lubrication therapies used in other di-arthrodial joints to restore native healthy friction coefficients have been considered as potential alternatives [7–11]. However, the TMJ is a ginglymodiarthrodial joint and contains fibrocartilage (not hyaline) covering the articular surface [12]. The TMJ also contains a unique disc that separates the temporal fossa from the mandibular condyle to redistribute loads and facilitate sliding (Fig 1A). A more thorough understanding of the tribology of native healthy TMJ cartilage will identify therapeutic targets that could enhance the development of lubrication therapies for TMJ disease.

Only a handful of studies have measured the friction coefficients of tissues from the TMJ. These studies have shown that friction in the TMJ can change due to fluid pressurization, anatomic location, and sliding direction[13–17]. Pendulum devices, used to measure friction coefficients of the intact TMJ, have shown that whole joint friction increases with increasing loading duration[13,14]. This increase in friction is linked to fluid exudation from the articular cartilage and disc [15]. Additional studies, which measured friction using migrating contact areas, have shown friction coefficients of condyles decreases with increases in speed and the Peclet number [16,17]. The disc also showed decreases in friction coefficient with increases in sliding speed [16,17]. In addition to speed, these changes in friction coefficient were dependent on the sliding direction of the condyle and disc, where medial-lateral (ML, orthogonal to the fiber direction) resulted in larger friction coefficients than anterior-posterior sliding [16]. These studies indicate TMJ cartilaginous tissues exhibit changes in friction coefficients due to fluid

pressurization at the tissue surface and fiber orientation. However, these friction tests have not determined how varying amounts of fluid pressurization, the tissue sliding direction, and the anatomic location of mandibular condyles and discs interact and change the observed friction coefficient.

The Stribeck framework is a useful tool for understanding mechanisms of lubrication [18–22]. Although originally developed for hard materials and journal bearings[23], this approach has more recently been modified to identify friction modes for cartilage (boundary mode friction, mixed mode, and elastoviscous friction mode)[18–22]. The Stribeck curve identifies these modes by plotting friction coefficient as a function of the dimensionless Sommerfeld number, S.

$$S = \frac{\eta * v * w}{P} \quad (1)$$

The Sommerfeld number is calculated as the product of the fluid viscosity (η), the sliding speed (v), and the sample width (w) divided by the normal load (P). Boundary mode friction is characterized by high friction coefficients due to the direct contact of the two sliding surfaces. In contrast, elastoviscous mode is associated with the lowest friction coefficient and the most fluid pressure at the tissue surface. Mixed mode is the transition from boundary mode to elastoviscous mode, where friction coefficient decreases with increases in speed, increases in fluid viscosity and/or decreases in normal load. This Stribeck framework has been documented for hyaline cartilage from the knee[18,20], and ankle[24] and is particularly useful to calculate the boundary friction, elastoviscous friction mode, and transition number (mixed mode). However, this framework has not been applied to cartilage from the TMJ.

Journal of Biomechanical Engineering. Received April 25, 2019;
Accepted manuscript posted October 28, 2019. doi:10.1115/1.4045283

A number of factors are likely to affect TMJ cartilage lubrication. The thick collagen fibers on the surface of the mandibular condyle and disc could cause the friction coefficient to change based on the sliding direction of the sample[25]. Additionally, these surface fibers, their orientation, and concentration of boundary lubricants change based on anatomic location in both the mandibular condyle and disc [26,27]. As a result of these surface properties, this study will identify 1) if the Stribeck curve framework accurately describes the lubrication of mandibular condyles and discs and 2) if each boundary friction, elastoviscous friction, and transition friction mode changes based on sliding direction and anatomic location.

Methods

Cartilage and disc removal

The mandibular condyle and disc were removed from both the left and the right side of 7 porcine heads (6 heads for condyle analysis and 5 heads for disc analysis) obtained from a local butcher (Shrader Meats, Romulus, NY, Fig 1A). The animals were of mixed breed and unknown sex, with an average age of 6 to 7 months. During joint dissection, the inferior TMJ capsule was preserved with the disc attached to the condyle. Discs were carefully removed from the surface of the condyle and a 5 mm diameter biopsy punch was used to harvest samples from 4 anatomic regions of the disc (medial, lateral, anterior, posterior, Fig 1B). The anterior posterior (AP) direction was marked on all disc samples. A total of 32 samples were taken from TMJ discs, with 8 samples at each of the 4 anatomic locations (medial, lateral, anterior, and posterior, Fig 1B). All samples were frozen immediately after joint dissection. Prior to testing samples were thawed at room temperature in phosphate buffer saline (PBS, Corning Cellgro, Manassas, VA). The total thickness of each sample was measured with a micrometer and recorded. The inferior aspect of

the disc (i.e. the surface in contact with the condyle) was later slid in both the anterior-posterior (AP, along the fibers) and the medial-lateral (ML, against the fibers) directions.

To verify fiber directions in the TMJ discs, second harmonic generation microscopy was used as described previously[28]. Images of collagen fibers were obtained using a Zeiss LSM 880 confocal/multiphoton inverted microscope with a 40x/1.2 C-Apochromat water immersion objective at wavelengths between 437-464 nm.

Mandibular condyles were obtained by taking a 6 mm diameter biopsy punch at 5 anatomic regions of the joint (medial, lateral, anterior, posterior, and central, Fig 1B). Since the condylar cartilage layer was very thin, each punch contained both cartilage and bone. Once removed from the joint, each osteochondral condyle sample was cut to a thickness of 2 mm. The anterior posterior (AP) direction on each sample was marked to keep track of the sliding direction. A total of 40 condyle samples were slid in both the AP and ML directions with 8 samples from each of the 5 anatomic locations.

Dextran formation and viscosity measurements

To obtain a large span of viscosities, several concentrations of dextran were used. Increasing concentrations of dextran in solution increases the fluid viscosity and has previously been shown to provide similar Stribeck curves to those generated by solutions of hyaluronic acid at similar viscosities[20]. Dextran solutions were made by mixing 20 MDa dextran (Sigma Aldrich, St. Louis, MO) with PBS at concentrations of 0%, 9%, and 23% (w/v). The viscosity of these solutions was determined using a commercial rheometer (Discovery Hybrid Rheometer 3, TA instruments, New Castle, DE) as previously described [20]. Viscosity measurements were measured using a 40 mm cone-plate geometry with a 2º angle, and viscosity values were taken at

a shear rate of $\dot{\gamma} = 1\ s^{-1}$. This shear rate resulted in viscosity values of 1, 31.5 and 218 mPa-s for 0%, 9% and 23% dextran concentrations respectively.

Friction coefficient measurements

Friction coefficients were measured using a custom cartilage-on-glass tribometer[18,19], as previously described. Briefly, samples were slid at speeds that spanned 2 orders of magnitude and in viscosities that spanned 2 orders of magnitude, generating conditions that spanned 4 orders of magnitude in the Sommerfeld number (S, Eq. (1)). Half the samples were tested in the AP direction first and half were tested in the ML direction first (Fig 1C). Each sample was placed in 0% dextran, compressed, and allowed to relax for at least 30 minutes and until an equilibrium load of 100g (35 kPa) for the condyle and 60g (30 kPa) for the disc was obtained. Once equilibrium was reached, samples were slid at 9 different speeds that spanned two orders of magnitude (0.1, 0.3, 0.5, 0.7, 1.0, 3.0, 5.0, 7.0, and 10 mm/s). During sliding, a biaxial load cell measured the instantaneous normal and shear loads, from which the friction coefficient was calculated.

After sliding in 0% dextran, the sample was removed from the tribometer and placed in PBS, while the media wells were cleaned to prevent any contamination from the previous test. Then, samples were placed back in the tribometer in 9% dextran and tested in the same sliding direction at the same 9 sliding speeds. This process was repeated for the 23% dextran solution (Fig 1D). Then, the sample was turned 90° and slid in the orthogonal direction using the same process of compressing, relaxing, and sliding in 3 concentrations of dextran at 9 sliding speeds (Fig 1E).

To obtain Stribeck curves and identify friction modes, all data for each sample slid in a given direction was plotted against the Sommerfeld number, a dimensionless number traditionally used to explain tribological phenomena. The Sommerfeld number, S, was calculated from Eq. (1). The friction coefficients versus the Sommerfeld number for each anatomic location and sliding direction was then fit to a Stribeck curve with the following equation[20]:

$$\mu(s) = \mu_{min} + (\mu_{b-}\mu_{min})e^{-\left(\frac{S}{S_t}\right)^d} \quad (2)$$

In this equation, μ_{min} represents the elastoviscous (minimum) friction coefficient, μ_b is the boundary mode friction coefficient, S_t is the transition number between boundary and elastoviscous mode, and d indicates the slope of the curve between boundary and elastoviscous mode friction. These four parameters (μ_{min}, μ_b, S_t, and d) were obtained by minimizing the error between predicted and measured friction coefficients using a least-squares fitting algorithm in Matlab (Mathworks, Natick, MA). All fitting parameters were constrained to be greater than zero with initial guesses ranging from of 0.03, 0.2, 1, and 2 for μ_{min}, μ_b, S_t, and d respectively.

Statistics

Stribeck curves were analyzed for goodness of fit using an R^2 parameter and a root mean square error (RMSE). Differences in friction coefficients based on anatomic location and sliding direction for the disc and condyles were analyzed separately using a linear random effects model in R Studio (RStudio, Boston, MA). The random effects of this model accounted for variability between pigs, multiple samples from a single head (ie: left and right side), the repeated testing of samples in both the AP and ML direction, and the initial sliding direction. Differences between

groups were calculated using a Tukey post-hoc analysis and were considered statistically significant based on a p value of less than 0.05.

Results

The friction coefficient of mandibular condyles and discs decreased with increases in sliding speed. These changes in friction coefficient were largest in the highest fluid viscosity for all sliding directions and anatomic locations. When tissue was slid in PBS, the lowest viscosity fluid, very small decreases in friction coefficient were observed with increases in sliding speed (Fig 2A, 3A). In 9% dextran, friction coefficients dropped by a factor of 2 while the sliding speed changed from 0.1 mm/s to 10 mm/s (Fig 2B, 3B). In the highest viscosity fluid (23% dextran), the friction coefficients dropped by almost an order of magnitude as sliding speed increased (Fig 2C, 3C). These decreases in friction coefficient occurred in both sliding directions for all anatomic location as viscosity and sliding speed increased.

For all condyle and disc samples, plotting the friction coefficient versus the Sommerfeld number showed clear Stribeck curve behavior (Fig 4). These Stribeck curve fits (Eq. (2)) yielded high R^2 values (R^2 range 0.90 – 0.97 and 0.87 – 0.95 for condyle and disc respectively) and low RMSE, (RMSE range 0.011 – 0.0195 and 0.016 - 0.023 for condyle and disc respectively) in all TMJ tissues, at all anatomic locations, and all sliding speeds. The friction coefficients of condyles and discs in boundary mode (μ_b = 0.17 – 0.22) were almost an order of magnitude higher than the elastoviscous friction (μ_{min} = 0.009 – 0.03) at all anatomic locations and sliding directions. The transition number ranged from 7.4×10^{-6} to 38×10^{-6} for all samples. This approach enabled direct measurements of the boundary friction, minimum friction, and transition number of TMJ tissues.

Journal of Biomechanical Engineering. Received April 25, 2019;
Accepted manuscript posted October 28, 2019. doi:10.1115/1.4045283

The Stribeck curve fit coefficients of condyles changed based on anatomic location. The boundary friction coefficient of mandibular condyles was highest in the anterior and central regions (μ_b~0.21 and μ_b~0.22 respectively, Fig 5A). The posterior region of the condyle showed the lowest boundary friction coefficient and the largest differences when compared to the other anatomic locations (μ_b~0.17, Fig 5D), but no significant differences were reported. The elastoviscous friction coefficient of mandibular condyles was lowest in the posterior region (μ_{min}~0.009) but showed no statistical significance when compared to all other regions (Fig 5B, Fig 5E, μ_{min}~0.013 to 0.019 for all other anatomic regions). The transition number of mandibular condyles was almost two times larger in the anterior and posterior regions ($S_t \sim 22x10^{-6}$ and $S_t \sim 19x10^{-6}$ respectively) than both the lateral ($S_t \sim 11x10^{-6}$) and central regions ($S_t \sim 9.4x10^{-6}$, Fig 5C, 5F, $p < 0.05$ between the anterior and central regions, $p = 0.05$ between anterior and lateral regions). When compared to other anatomic locations, the posterior region of the mandibular condyle consistently had the lowest friction coefficient for multiple lubricating modes.

Similar to the mandibular condyles, TMJ discs showed changes in the friction modes based on anatomic location. The lateral region had the lowest boundary friction coefficient (μ_b = 0.17, Fig 6A, 6D). All other anatomic regions had boundary friction coefficients that were 10-30% higher ($p = 0.10$, 0.17, & 0.40 for the lateral region vs. the posterior, anterior and medial region respectively, Fig 6D). The anterior and posterior regions consistently showed the lowest elastoviscous friction coefficients (μ_{min}~0.011). The lateral region consistently showed the highest friction coefficient, which approached significance against the anterior region (Fig 6B, Fig 6E, $p = 0.09$). The transition from boundary friction to elastoviscous friction did not change based on anatomic location (Fig 6C, Fig 6F).

Both tissues showed some small changes in friction due to the sliding direction, and no significant differences. The condyle central region showed a 20% higher boundary friction coefficient and a 60% lower transition number in the AP direction than the ML direction (Fig 5A). These differences approached statistically significance (Fig 7, $p = 0.08$). In the disc, 3 out of 4 anatomic locations resulted in 10% to 20% higher boundary friction coefficient due to sliding ML instead of AP (Fig 6A). However, no statistical significance was found based on sliding direction (Table 1). The elastoviscous friction coefficient of the lateral and medial regions of the disc was 20% higher due to sliding in the ML direction rather than the AP direction (Fig 6B, Table 1). The other friction modes of the condyle and disc showed little to no differences based on sliding direction. Overall changing the sliding direction of each sample resulted in small changes in friction coefficients that were not statistically significant or consistent between anatomic locations.

When the friction modes of the condyle and disc were compared, the lateral region and the transition number showed the largest differences (Table 2). The lateral region of the disc had a 15% lower boundary friction coefficient, 2 times larger elastoviscous friction coefficient, and a 3 times larger transition number than the mandibular condyle in that same region (lateral). Similarly, the disc showed higher transition numbers (~2-3 times larger) than the condyle in all anatomic regions except the anterior. These differences between the disc and the condyle indicate the two tissues behave differently at the same Sommerfeld number.

Discussion

The objectives of this study were to determine if TMJ condylar cartilage and discs followed Stribeck curve behavior and to determine any differences between these curves based on anatomic location and sliding direction. Both tissues from all anatomic locations followed

Stribeck curve behavior as indicated by the presence of multiple friction modes. The observed Stribeck curves were not identical for all anatomic locations. Very few differences in friction coefficients based on sliding direction were observed. These results identify differences in friction behavior based on anatomic location, sliding direction, and the friction mode, which were previously unknown for the mandibular condyle and disc.

Boundary friction coefficients have been correlated with multiple factors, including the surface roughness of the tissue. Because the surface roughness of the condyles are similar to the disc[16], we expected these two tissues to have similar boundary mode friction coefficients. Overall, the condyle and disc did have similar boundary mode friction coefficients. Additionally, the surface roughness of the mandibular condyles is higher than hyaline cartilage of other joints, and was expected to result in a larger boundary friction coefficient[11]. Unexpectedly, the boundary friction coefficient of mandibular condyles in this study was lower than hyaline cartilage of other joints[18,20,24,29]. Other surface characteristics known to affect boundary lubrication such as lubricin concentration could cause the differences observed between mandibular condyles and hyaline cartilage. Both mandibular condyles and hyaline condylar cartilage have a high concentration of lubricin, a boundary lubricant, on their tissue surface[11,30]. These previous studies use immunohistochemical staining to visualize lubricin. Since this approach is inherently non-quantitative, it would be important in future work to directly quantify lubricin content on TMJ tissues.

The presence of a rough, oriented fibrous surface in these tissues was expected to result in large differences based on sliding direction. This thought was based on previous findings that the friction coefficients of mandibular condyles and discs changed based on sliding direction[16]. This previous study was performed using migrating contact areas, which would

Journal of Biomechanical Engineering. Received April 25, 2019;
Accepted manuscript posted October 28, 2019. doi:10.1115/1.4045283

most likely result in friction coefficient in the elastoviscous friction mode at high Sommerfeld numbers [31–33]. In contrast to previous work, we saw no significant changes in elastoviscous friction or any other friction mode due to sliding direction. If the circumferential orientation of the fibers on the edges of the TMJ disc and mandibular condyles are considered[34,35], sliding in the medial lateral direction should have resulted in higher friction coefficients for the anterior and posterior direction. However, this study did not observe these differences and noted no statistical significance based on sliding direction (some anatomic regions approached statistical significance, Table 1). This finding may be explained by examining the fiber directions on the surface of the samples (supplemental figures). Friction coefficients were not affected by the sliding direction or the fiber orientation in this study.

Using Stribeck curves, this study showed discs have a higher transition numbers than mandibular condyles (Fig 8), and the mandibular condyles had a higher transition number than articular hyaline cartilage of other joints[20]. Stribeck curves make these comparisons possible because of the use of the dimensionless Sommerfeld number, which provides the ability to directly compare friction coefficients of tissues that may have been tested under slightly different conditions[20]. This pattern of transition numbers indicates it is more difficult to pressurize fluid on the surface of TMJ cartilage than in other joints containing hyaline cartilage. This phenomenon could be a result of the high surface permeability of mandibular condyles and the higher permeability of the TMJ disc[31,32]. A more permeable surface requires a larger amount of fluid flow to adequately pressurize fluid at the surface. In addition to transition number, the elastoviscous friction coefficients are lower in the TMJ (μ_{min}~0.009 to 0.19), than hyaline cartilage of other joints (μ_{min}~0.045 to 0.06) [16,20,36]. Also confirming that more fluid is pressurized at the surface of the mandibular condyle than in hyaline cartilage operating under

elastoviscous friction mode. The increase in transition number of mandibular condyles and discs could indicate that these tissues are more likely to operate in boundary mode friction at physiologic sliding speeds (~40mm/s)[37]. These differences in cartilage behavior could also indicate therapeutic injections might require a more viscous lubricant to reach elastoviscous friction coefficients.

Interesting the lateral region of the disc had both the lowest boundary friction coefficient recorded in this study and is the first region in the TMJ to exhibit signs of damage [38]. Previous work using finite element models have shown this damage prior to disease could be due to the large stress and strain concentrated in the lateral zone of the disc [39,40] during normal joint movement. These large stresses indicate large normal loads and the potential for low fluid pressurization at the tissue surface, and more time under boundary mode friction. The healthy joint may have developed the ability to protect the lateral region of the disc from damage by localizing the lowest boundary friction coefficients in the region most likely to see tissue damage. To prevent TMJ disease, lubrication therapies may need to focus on restoring this ultra-low boundary friction coefficient using regenerative medicine techniques such as HA or lubricin injections[8,9,41] or regenerative medicine technologies[11,42–44].

While this study has direct implications to understanding the lubricating mechanisms of the mandibular condyle and disc, there are several limitations that must be considered. First, this study uses porcine TMJ cartilage, which is not identical to humans. However, the porcine TMJ is one of the most commonly used animal models for TMJ research, because the joint morphology, internal structures (e.g. disc biochemical properties and compressive modulus) and attachments are similar to humans [45–47]. Additionally, a post processing power analysis revealed that some changes in the friction modes based on anatomic location were underpowered (supplemental,

table 1). An increase in sample size may increase statistical power and result in more statistically significant differences based on anatomic location, but it's unlikely the magnitude differences will change drastically. Finally, friction coefficients in this study were plotted against the Sommerfeld number, which is a function of sliding speed, viscosity, and normal loads. The normal loads were not changed in this study. However, previous work using knee articular cartilage shows that altering normal loads scales friction coefficients as expected from the Stribeck framework. Future work involving changes to the normal loads of these tissues may solidify this system and these results for healthy mandibular condyles and discs.

This study provided insight into the friction coefficients required for healthy TMJ function. We observed differences in friction coefficients based on anatomic location, which implies multiple surface characteristics are also changing based on anatomic location. No differences based on sliding direction were observed, implying the orientation of the surface fibers may not greatly affect the friction coefficient. Similar to other cartilaginous tissues, the Stribeck framework accurately explains changes in the friction coefficients of TMJ cartilage, therefore some lubrication therapies that increase fluid viscosity may be effective in treating TMJ disorders. However, the observed friction coefficients of the fibrocartilaginous TMJ tissues were less than hyaline cartilage and the transition number was higher than hyaline cartilage in other joints. Therefore, some hyaline cartilage lubrication therapies may need to be modified (more lubricin, higher viscosities, etc.) to treat TMJ diseases and restore joint function.

Acknowledgements

The authors would like to thank Sierra Cook and Professor Itai Cohen for the assistance in rheology testing. We also thank Marianne Lintz for the TMJ schematic and SHG images.

Funding

This project was funded by NSF GRFP (DGE-1650441), Cornell Center for Materials Research (CCMR), and the following NSF grants (DMR - 1460428 and DMR – 1719875, CMMI 1927197).

References

[1] Solberg, W. K., Woo, M. W., and Houston, J. B., 1979, "Prevalence of Mandibular Dysfunction in Young Adults," J. Am. Dent. Assoc., **98**(1), p. 25—34.

[2] Murphy, M. K., Macbarb, R. F., Wong, M. E., and Athanasiou, K., 2013, "Temporomandibular Joint Disorders: A Review of Etiology, Clinical Management, and Tissue Engineering Strategies," Int J Oral Maxillofac Implant., **28**(6), pp. 393–414.

[3] Bodine, T. P., Wolford, L. M., Araujo, E., Oliver, D. R., and Buschang, P. H., 2016, "Surgical Treatment of Adolescent Internal Condylar Resorption (AICR) with Articular Disc Repositioning and Orthognathic Surgery in the Growing Patient — a Pilot Study," Prog. Orthod., **17**(2), pp. 1–7.

[4] Nitzan, D. W., 2001, "The Process of Lubrication Impairment and Its Involvement in Temporomandibular Joint Dics Displacement. A Theoretical Concept," J. Oral Maxillofac. Surg., **59**(1), pp. 36–45.

[5] Stegenga, B., 2010, "Nomenclature and Classification of Temporomandibular Joint Disorders," Oral Rehabil., **37**, pp. 760–765.

[6] Koolstra, J. H., 2012, "Biomechanical Analysis of the Influence of Friction in Jaw Joint Disorders," Osteoarthr. Cartil., **20**(1), pp. 43–48.

[7] Goldberg, V. M., and Buckwalter, J. A., 2005, "Hyaluronans in the Treatment of Osteoarthritis of the Knee : Evidence for Disease-Modifying Activity," Osteoarthr. Cartil., **13**, pp. 216–224.

[8] Jay, G. D., Fleming, B. C., Watkins, B. A., Mchugh, K. A., Anderson, S. C., Zhang, L. X., Teeple, E., Waller, K. A., and Elsaid, K. A., 2010, "Prevention of Cartilage Degeneration and Restoration of Chondroprotection by Lubricin Tribosupplementation in the Rat Following Anterior Cruciate Ligament Transection," Arthritis Rheumatol., **62**(8), pp. 2382–2391.

[9] Flannery, C. R., Zollner, R., Corcoran, C., Jones, A. R., Root, A., Rivera-Bermúdez, M. A., Blanchet, T., Gleghorn, J. P., Bonassar, L. J., Bendele, A. M., Morris, E. A., and Glasson, S. S., 2009, "Prevention of Cartilage Degeneration in a Rat Model of Osteoarthritis by Intraarticular Treatment with Recombinant Lubricin," Arthritis Rheum., **60**(3), pp. 840–847.

[10] McNary, S. M., Athanasiou, K. A., and Reddi, A. H., 2012, "Engineering Lubrication in Articular Cartilage.," Tissue Eng. Part B. Rev., **18**(2), pp. 88–100.

[11] Tanaka, E., Detamore, M. S., Tanimoto, K., and Kawai, N., 2008, "Lubrication of the Temporomandibular Joint," Ann. Biomed. Eng., **36**(1), pp. 14–29.

[12] Wadhwa, S., and Kapila, S., 2008, "TMJ Disorders: Future Innovations in Diagnostics and Therapeutics," J. Dent. Educ., **72**(8), pp. 930–947.

[13] Tanaka, E., Kawai, N., Tanaka, M., Todoh, M., Van Eijden, T., Hanaoka, K., Dalla-Bona, D. A., Takata, T., and Tanne, K., 2004, "The Frictional Coefficient of the Temporomandibular Joint and Its Dependency on the Magnitude and Duration of Joint Loading," J. Dent. Res., **83**(5), pp. 404–407.

[14] Nickel, J. C., and McLachlan, K. R., 1994, "In Vitro Measurement of the Stress-Distribution Properties of the Pig Temporomandibular Joint Disc," Arch. Oral Biol., **39**(5), pp. 439–448.

[15] Forster, H., and Fisher, J., 1999, "The Influence of Continuous Sliding and Subsequent Surface Wear on the Friction of Articular Cartilage," Proc Instn Mech. Engrs, **213**(H), pp. 329–345.

[16] Zimmerman, B. K., Bonnevie, E. D., Park, M., Zhou, Y., Wang, L., Burris, D. L., and Lu, X. L., 2015, "Role of Interstitial Fluid Pressurization in TMJ Lubrication," J. Dent. Res., **94**(1), pp. 85–92.

[17] Ruggiero, L., Zimmerman, B. K., Park, M., Han, L., Wang, L., Burris, D. L., and Lu, X. L., 2015, "Roles of the Fibrous Superficial Zone in the Mechanical Behavior of TMJ Condylar Cartilage," Ann. Biomed. Eng., **43**(11), pp. 2652–2662.

[18] Gleghorn, J. P., and Bonassar, L. J., 2008, "Lubrication Mode Analysis of Articular Cartilage Using Stribeck Surfaces," J. Biomech., **41**(9), pp. 1910–1918.

[19] Gleghorn, J. P., Jones, A. R. C., Flannery, C. R., and Bonassar, L. J., 2007, "Boundary Mode Frictional Properties of Engineered Cartilaginous Tissues," Eur. Cells Mater., **14**, pp. 20–28.

[20] Bonnevie, E. D., Galesso, D., Secchieri, C., Cohen, I., and Bonassar, L. J., 2015, "Elastoviscous Transitions of Articular Cartilage Reveal a Mechanism of Synergy between Lubricin and Hyaluronic Acid.," PLoS One, **10**(11), p. e0143415.

[21] Shi, L., Sikavitsas, V. I., and Striolo, A., 2011, "Experimental Friction Coefficients for Bovine Cartilage Measured with a Pin-on-Disk Tribometer: Testing Configuration and Lubricant Effects," Ann. Biomed. Eng., **39**(1), pp. 132–146.

[22] Feeney, E., Peal, B. T., Inglis, J. E., Su, J., Nixon, A. J., Bonassar, L. J., and Reesink, H. L., 2019, "Temporal Changes in Synovial Fluid Composition and Elastoviscous Lubrication in the Equine Carpal Fracture Model," J. Orthop. Res., pp. 1–9.

[23] Hersey, M. D., 1914, "Laws of Lubrication.," J. Washingt. Acad. Sci., **4**, pp. 542–552.

[24] Henak, C. R., Ross, K. A., Bonnevie, E. D., Fortier, L. A., Cohen, I., Kennedy, J. G., and Bonassar, L. J., 2016, "Human Talar and Femoral Cartilage Have Distinct Mechanical Properties near the Articular Surface," J. Biomech., **49**(14), pp. 3320–3327.

[25] Singh, M., and Detamore, M. S., 2009, "Biomechanical Properties of the Mandibular Condylar Cartilage and Their Relevance to the TMJ Disc," J. Biomech., **42**(4), pp. 405–417.

[26] Kim, K.-W., Wong, M. E., Helfrick, J., Thomas, J., and Athanasiou, K. A., 2003, "Biomechanical Tissue Characterization of the Superior Joint Space of the Porcine Temporomandibular Joint," Ann. Biomed. Eng., **31**, pp. 924–930.

[27] Hu, K., Radhakrishnan, P., Patel, R. V, and Mao, J. J., 2001, "Regional Structural and Viscoelastic Properties of Fibrocartilage upon Dynamic Nanoindentation of the Articular Condyle," J. Struct. Biol., **136**(1), pp. 46–52.

[28] McCorry, M. C., Kim, J., Springer, N., Sandy, J., Plaase, A., and Bonassar, L. J., 2019, "Regulation of Proteoglycan Production by Varying Glucose Concentrations Controls Fiber Formation in Tissue Engineered Menisci," Acta Biomater.

[29] Middendorf, J. M., Griffin, D. J., Shortkroff, S., Dugopolski, C., Kennedy, S., Siemiatkoski, J., Cohen, I., and Bonassar, L. J., 2017, "Mechanical Properties and Structure-Function Relationships of Human Chondrocyte-Seeded Cartilage Constructs after in Vitro Culture," J. Orthop. Res., pp. 1–9.

[30] Tanimoto, K., Kamiya, T., Tanne, Y., Kunimatsu, R., Mitsuyoshi, T., Tanaka, E., and Tanne, K., 2011, "Superficial Zone Protein Affects Boundary Lubrication on the Surface of Mandibular Condylar Cartilage," Cell Tissue Res., **344**(2), pp. 333–340.

[31] Burris, D. L., and Moore, A. C., 2017, "Cartilage and Joint Lubrication: New Insights Into the Role of Hydrodynamics," Biotribology, **12**(May), pp. 8–14.

[32] Moore, A. C., and Burris, D. L., 2017, "Tribological Rehydration of Cartilage and Its Potential Role in Preserving Joint Health," Osteoarthr. Cartil., **25**(1), pp. 99–107.

[33] Caligaris, M., and Ateshian, G. A., 2008, "Effects of Sustained Interstitial Fluid Pressurization under Migrating Contact Area, and Boundary Lubrication by Synovial Fluid, on Cartilage Friction," Osteoarthr. Cartil., **16**(10), pp. 1220–1227.

[34] Detamore, M. S., and Athanasiou, K. A., 2003, "Structure and Function of the Temporomandibular Joint Disc: Implications for Tissue Engineering," J. Oral Maxillofac. Surg., **61**(4), pp. 494–506.

[35] Scapino, R., Canham, P., Finlay, H., and Mills, D., 1996, "The Behaviour of Collagen Fibres in Stress Relaxation and Stress Distribution in the Jaw Joint Disc of Rabbits," Arch. Oral Biol., **41**(11), pp. 1039–1052.

[36] Bonnevie, E. D., Baro, V. J., Wang, L., and Burris, D. L., 2011, "In Situ Studies of Cartilage Microtribology: Roles of Speed and Contact Area," Tribol. Lett., **41**(1), pp. 83–95.

[37] Gallo, L. M., Nickel, J. C., Iwasaki, L. R., and Palla, S., 2000, "Stress Field Translation in the Healthy Human Temporomandibular Joint," J. Dent Res, **79**(10), pp. 1740–1746.

[38] Werner, J. A., Tillmann, B., and Sehleieher, A., 1991, "Functional Anatomy of the Temporomandibular Joint: A Morphologic Study on Human Autopsy Material," Anat. Embryol, **183**, pp. 89–95.

[39] Beek, M., Koolstra, J. H., VanRuijven, L. J., and VanEijden, T. M. G. J., 2000, "Three-Dimensional Finite Element Analysis of the Human Temporomandibular Joint Disc," J. Biomech., **33**, pp. 307–316.

[40] Koolstra, J. H., and Van Eijden, T. M. G. J., 2005, "Combined Finite-Element and Rigid-Body Analysis of Human Jaw Joint Dynamics," J. Biomech., **38**(12), pp. 2431–2439.

[41] Guarda-Nardini, L., Stifano, M., Brombin, C., Salmaso, L., and Manfredini, D., 2007, "A One-Year Case Series of Arthrocentesis with Hyaluronic Acid Injections for Temporomandibular Joint Osteoarthritis," Oral Surgery, Oral Med. Oral Pathol. Oral Radiol. Endodontology, **103**(6), pp. 14–22.

[42] Wang, L., and Detamore, M. S., 2007, "Tissue Engineering the Mandibular Condyle.," Tissue Eng., **13**(8), pp. 1955–1971.

[43] Allen, K. D., and Athanasiou, K. A., 2006, "Viscoelastic Characterization of the Porcine Temporomandibular Joint Disc under Unconfined Compression," J. Biomech., **39**(2), pp. 312–322.

[44] Lowe, J., and Almarza, A. J., 2017, "A Review of In-Vitro Fibrocartilage Tissue Engineered Therapies with a Focus on the Temporomandibular Joint," Arch. Oral Biol., **83**(February), pp. 193–201.

[45] Bermejo, A., Gonzblez, O., and Gonzalez, J., 1993, "The Pig as an Animal Model for Experimentation on the Temporomandibular Articular Complex," Oral Surg Oral Med Oral Pathol., **75**(1), pp. 18–23.

[46] Kalpakci, K., Willard, V., Wong, M., and Athanasiou, K. A., 2011, "An Interspecies Comparison of the Temporomandibular Joint Disc," J. Dent Res, **90**(2), pp. 193–198.

[47] Štembírek, J., Kyllar, M., Putnová, I., Stehlík, L., and Buchtová, M., 2012, "The Pig as an Experimental Model for Clinical Craniofacial Research," Lab. Anim., **46**(4), pp. 269–279.

Journal of Biomechanical Engineering. Received April 25, 2019;
Accepted manuscript posted October 28, 2019. doi:10.1115/1.4045283

List of Table Captions:

Table 1: Statistical differences (p-values) between the 2 sliding directions (ML vs. AP)

Table 2: Statistical differences (p-values) between condyles and discs

Supplemental Table 1: Statistical power analysis of the friction mode based on anatomic locations.

Journal of Biomechanical Engineering. Received April 25, 2019;
Accepted manuscript posted October 28, 2019. doi:10.1115/1.4045283

List of Figure Captions

Figure 1: Friction testing process for all samples A) Anatomy of the TMJ B) Cylindrical samples are removed from either the condyle or the disc at a known anatomic location. C) Each sample starts by sliding in either the medial-lateral (ML) or anterior-posterior (AP) sliding direction. D) Samples are slid at 9 speeds in each of the 3 fluids. E) Samples are slid in the orthogonal direction and part D is repeated.

Figure 2: Mandibular condylar cartilage friction coefficients versus sliding speed in multiple viscosities of dextran. As sliding speed and dextran viscosity increases the coefficient of friction decreases. (medial = red, lateral = blue, anterior = black, posterior = yellow, central = green, N = 8)

Figure 3: TMJ disc friction coefficients versus sliding speed in multiple viscosities of dextran. As sliding speed and dextran viscosity increases the coefficient of friction decreases. (medial = red, lateral = blue, anterior = black, posterior = yellow, N = 8)

Figure 4: Stribeck curve fits for (A) mandibular condyles (R^2 range 0.90 – 0.97; RMSE range 0.011 – 0.0195) and (B) discs (R^2 range 0.87 – 0.95; RMSE range 0.016 - 0.023) in both the anterior posterior and the medial lateral directions. All data fit the Stribeck curves well ($p < 0.0001$, medial = red, lateral = blue, anterior = black, posterior = yellow, central = green, N = 8).

Figure 5: Mandibular condyle friction modes based on anatomic location and sliding direction A) boundary friction coefficient B) minimum friction coefficient C) transition number (** indicate $p < 0.05$ between anatomic location, * indicate $p < 0.1$ for anatomic regions, + indicate $p< 0.1$ based on a sliding direction at a given anatomic location; medial = red, lateral = blue, anterior = gray, posterior = yellow, central = green, N = 8). D-F) Statistical difference (p-value) between anatomic locations on the condyle. Colors range from dark red ($p < 0.001$) to dark blue ($p = 1.0$).

Figure 6: Disc friction modes based on anatomic location and sliding direction: A) boundary friction coefficient B) minimum friction coefficient C) transition number (* indicate $p < 0.1$ for anatomic regions; medial = red, lateral = blue, anterior = gray, posterior = yellow, central = green, N = 8). D-F) Statistical difference (p-value) between anatomic locations for both sliding directions on the disc. Colors range from dark red ($p < 0.001$) to dark blue ($p = 1.0$).

Supplemental Figure 1: Second harmonic generation (SHG) images of the surface of the TMJ discs. Medial, lateral, and anterior region contains fibers that are oriented in the anterior posterior

Journal of Biomechanical Engineering. Received April 25, 2019;
Accepted manuscript posted October 28, 2019. doi:10.1115/1.4045283

direction, while the posterior region contained fibers oriented more in the medial lateral direction. Fibers and orientations were the least distinct in the medial region of the disc.

Supplemental Figure 2: Second harmonic generation (SHG) images of the surface of the condyles. All regions contained fibers. The fibers in the anterior region of the condyle appeared to be oriented more in the anterior posterior direction than the other regions of the condyle.

Journal of Biomechanical Engineering. Received April 25, 2019;
Accepted manuscript posted October 28, 2019. doi:10.1115/1.4045283

Tables

Table 1: Statistical differences (p-values) between the 2 sliding directions (ML vs. AP)

		Medial	Lateral	Anterior	Posterior	Central	Overall
Condyle	Boundary Friction	0.65	0.08	0.28	0.84	0.08	0.04
	Elastoviscous Friction	0.49	0.49	0.77	0.75	0.37	0.69
	Transition Number	0.98	0.29	0.11	0.94	0.49	0.81
Disc	Boundary Friction	0.25	0.53	0.10	0.25		0.25
	Elastoviscous Friction	0.22	0.56	0.84	0.99		0.32
	Transition Number	0.36	1.00	0.64	0.12		0.14

Colors range from dark red ($p < 0.001$) to dark blue ($p = 1.0$).

Journal of Biomechanical Engineering. Received April 25, 2019;
Accepted manuscript posted October 28, 2019. doi:10.1115/1.4045283

Table 2: Statistical differences (p-values) between condyles and discs

	Medial	Lateral	Anterior	Posterior	Overall
Boundary Friction	0.87	0.10	0.80	0.01	0.84
Elastoviscous Friction	0.55	0.16	0.41	0.80	0.90
Transition Number	0.27	0.00	0.81	0.08	0.01

Colors range from dark red ($p < 0.001$) to dark blue ($p = 1.0$).

Journal of Biomechanical Engineering. Received April 25, 2019;
Accepted manuscript posted October 28, 2019. doi:10.1115/1.4045283

Supplemental Table 1: Statistical power analysis of the friction mode based on anatomic locations.

		Statistical Power
Condyle	Boundary Friction	0.64
	Elastoviscous Friction	0.26
	Transition Number	0.96
Disc	Boundary Friction	0.64
	Elastoviscous Friction	0.68
	Transition Number	0.28

Colors range from dark red (P = 0) to dark blue (P = 0.8).

Journal of Biomechanical Engineering. Received April 25, 2019;
Accepted manuscript posted October 28, 2019. doi:10.1115/1.4045283

Figures

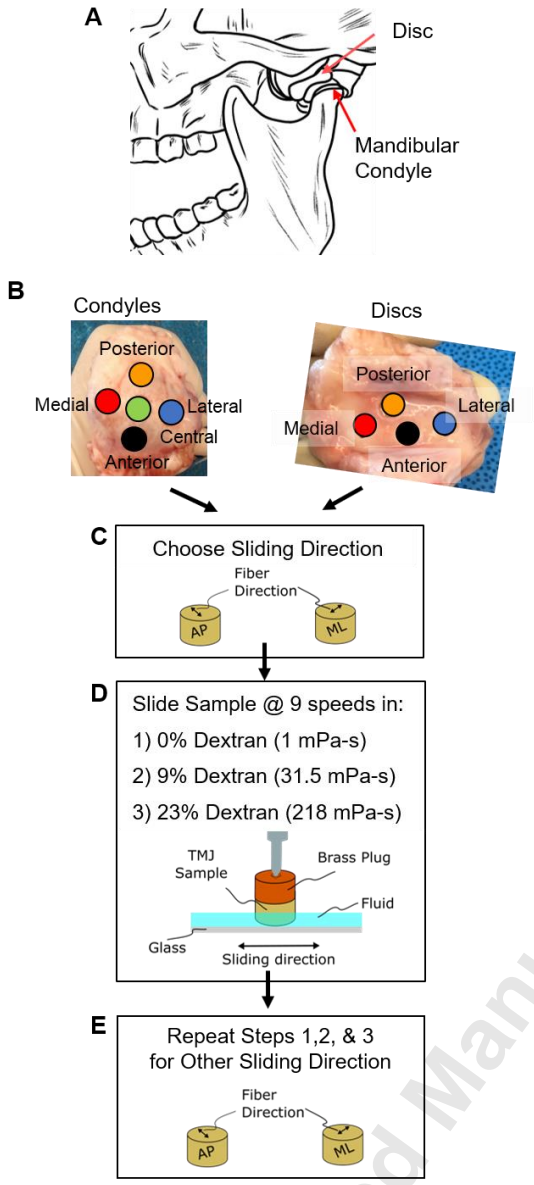

Figure 1: Friction testing process for all samples A) Anatomy of the TMJ B) Cylindrical samples are removed from either the condyle or the disc at a known anatomic location. C) Each sample starts by sliding in either the medial-lateral (ML) or anterior-posterior (AP) sliding direction. D) Samples are slid at 9 speeds in each of the 3 fluids. E) Samples are slid in the orthogonal direction and part D is repeated.

Journal of Biomechanical Engineering. Received April 25, 2019;
Accepted manuscript posted October 28, 2019. doi:10.1115/1.4045283

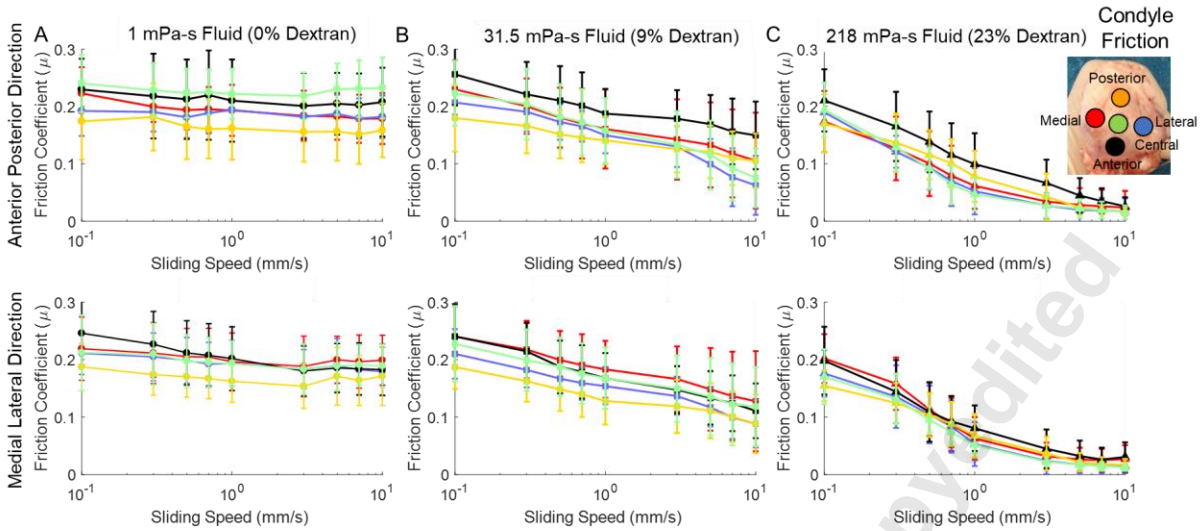

Figure 2: Mandibular Condylar cartilage friction coefficients versus sliding speed in multiple viscosities of dextran. As sliding speed and dextran viscosity increases the coefficient of friction decreases. (medial = red, lateral = blue, anterior = gray, posterior = yellow, central = green, N = 8)

Journal of Biomechanical Engineering. Received April 25, 2019;
Accepted manuscript posted October 28, 2019. doi:10.1115/1.4045283

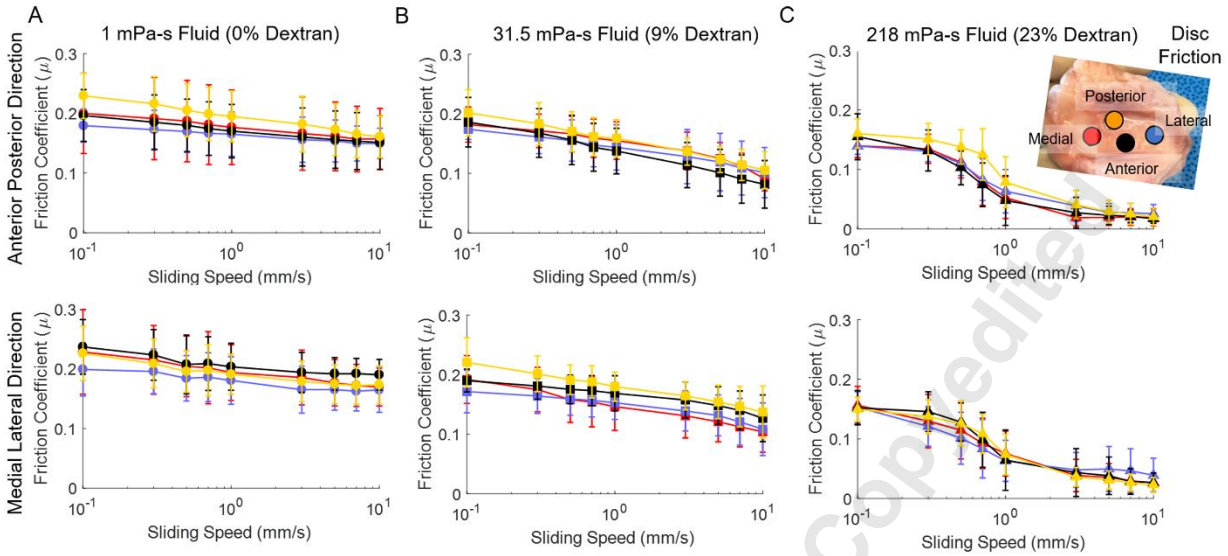

Figure 3: TMJ disc friction coefficients versus sliding speed in multiple viscosities of dextran. As sliding speed and dextran viscosity increases the coefficient of friction decreases. (medial = red, lateral = blue, anterior = black, posterior = yellow, N = 8)

Journal of Biomechanical Engineering. Received April 25, 2019;
Accepted manuscript posted October 28, 2019. doi:10.1115/1.4045283

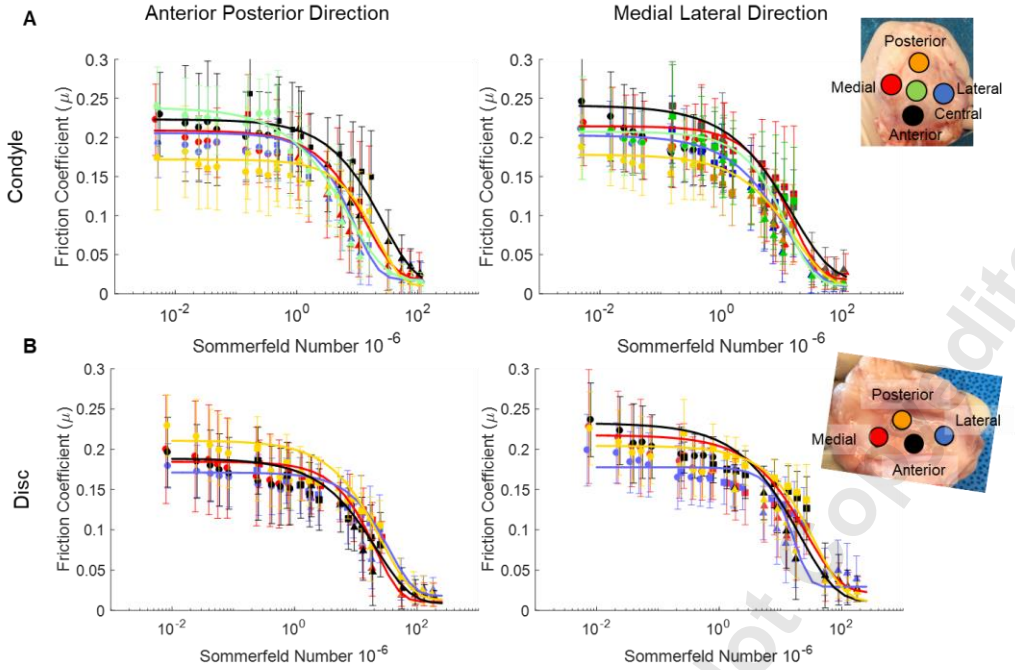

Figure 4: Stribeck curve fits for (A) mandibular condyles (R^2 range 0.90 – 0.97; RMSE range 0.011 – 0.0195) and (B) discs (R^2 range 0.87 – 0.95; RMSE range 0.016 - 0.023) in both the anterior posterior and the medial lateral directions. All data fit the Stribeck curves well ($p < 0.0001$, medial = red, lateral = blue, anterior = gray, posterior = yellow, central = green, N = 8).

Journal of Biomechanical Engineering. Received April 25, 2019;
Accepted manuscript posted October 28, 2019. doi:10.1115/1.4045283

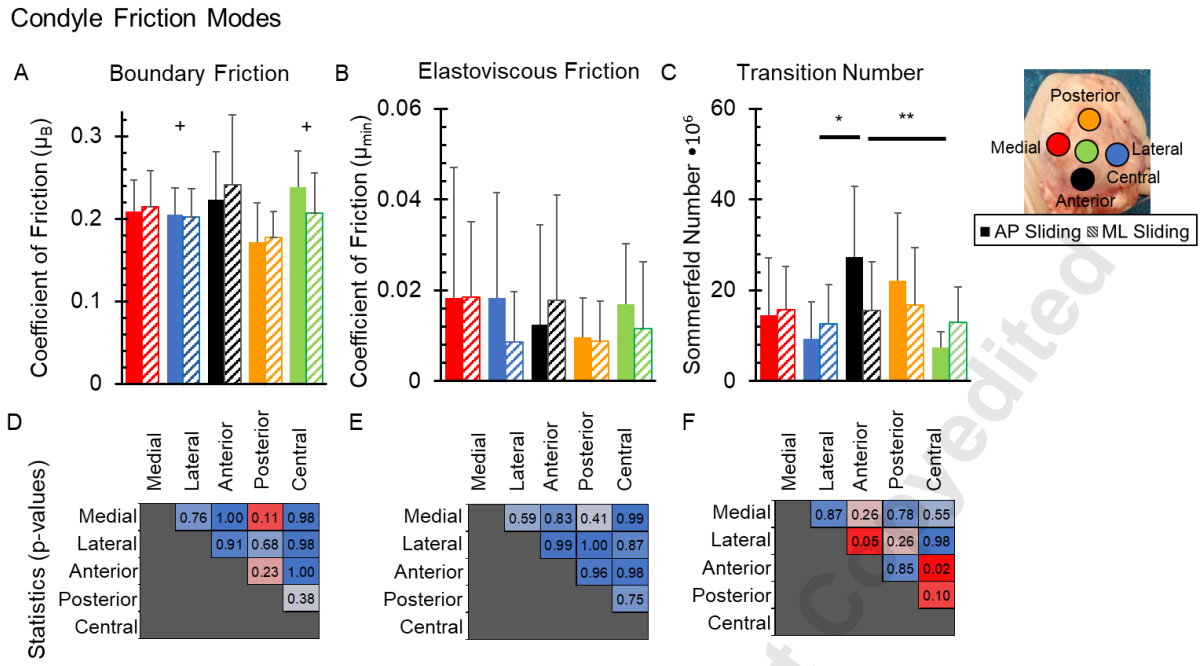

Figure 5: Mandibular condyle friction modes based on anatomic location and sliding direction A) boundary friction coefficient B) minimum friction coefficient C) transition number (** indicate $p < 0.05$ between anatomic location, * indicate $p < 0.1$ for anatomic regions, + indicate $p < 0.1$ based on a sliding direction at a given anatomic location; medial = red, lateral = blue, anterior = gray, posterior = yellow, central = green, N = 8). D-F) Statistical difference (p-value) between anatomic locations on the condyle. Colors range from dark red ($p < 0.001$) to dark blue ($p = 1.0$).

Journal of Biomechanical Engineering. Received April 25, 2019;
Accepted manuscript posted October 28, 2019. doi:10.1115/1.4045283

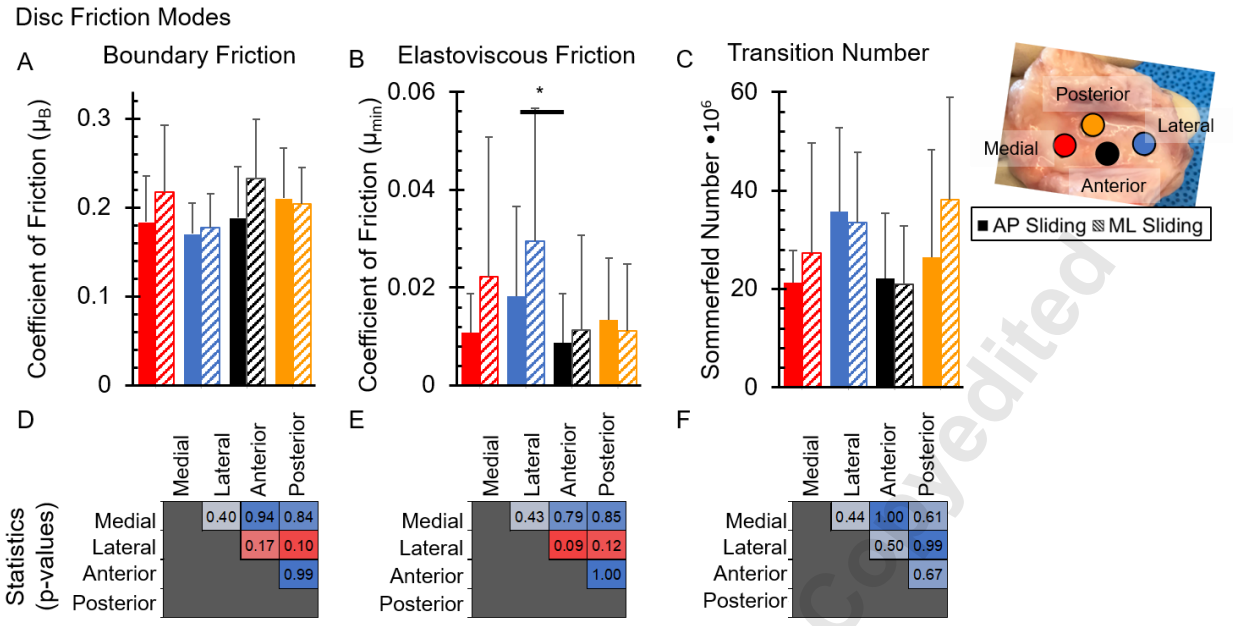

Figure 6: Disc friction modes based on anatomic location and sliding direction: A) boundary friction coefficient B) minimum friction coefficient C) transition number (* indicate $p < 0.1$ for anatomic regions; medial = red, lateral = blue, anterior = gray, posterior = yellow, central = green, N = 8). D-F) Statistical difference (p-value) between anatomic locations for both sliding directions on the disc. Colors range from dark red ($p < 0.001$) to dark blue ($p = 1.0$).

Journal of Biomechanical Engineering. Received April 25, 2019;
Accepted manuscript posted October 28, 2019. doi:10.1115/1.4045283

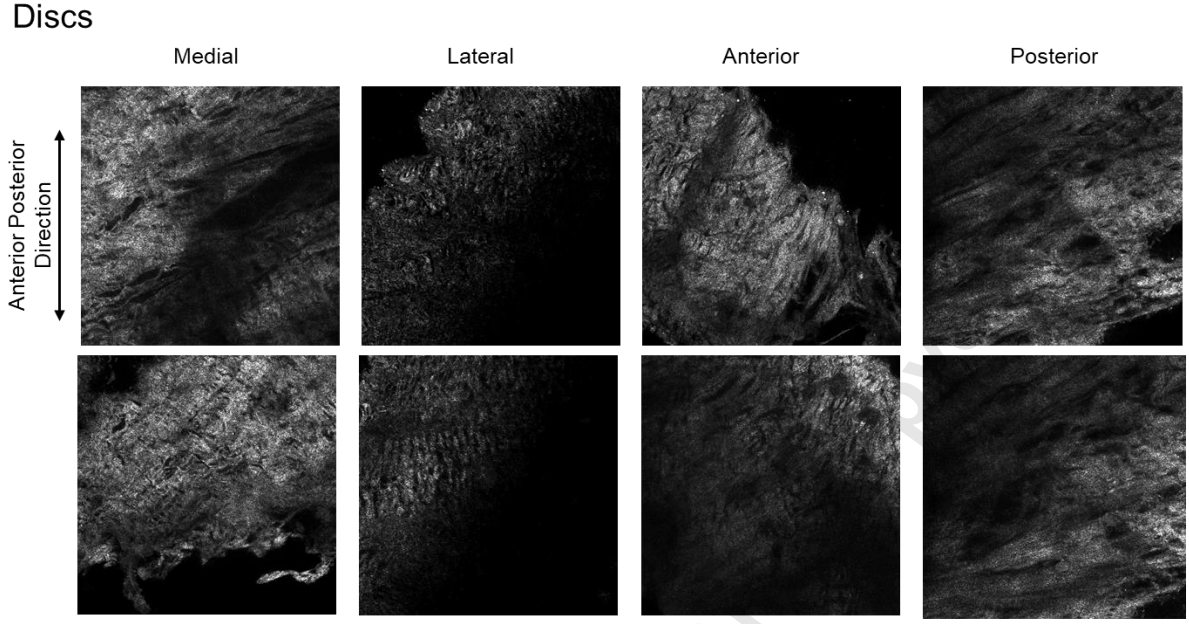

Supplemental Figure 1: Second harmonic generation (SHG) images of the surface of the TMJ discs. Medial, lateral, and anterior region contains fibers that are oriented in the anterior posterior direction, while the posterior region contained fibers oriented more in the medial lateral direction. Fibers and orientations were the least distinct in the medial region of the disc.

Journal of Biomechanical Engineering. Received April 25, 2019;
Accepted manuscript posted October 28, 2019. doi:10.1115/1.4045283

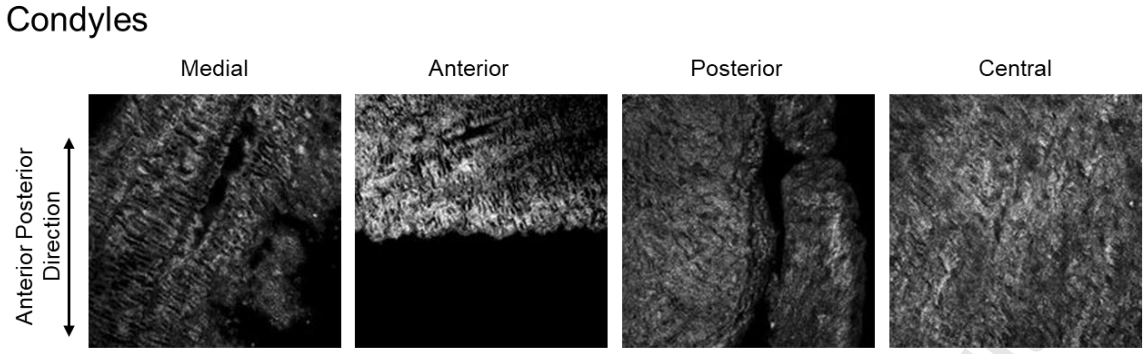

Supplemental Figure 2: Second harmonic generation (SHG) images of the surface of the condyles. All regions contained fibers. The fibers in the anterior region of the condyle appeared to be oriented more in the anterior posterior direction than the other regions of the condyle.